Stabilization of Three-Membered Rings by Protonation. The Cyclic Global Minimum of HP_2O^+, the Protonated Phosphorus Analogue of Nitrous Oxide

Randall D. Davy, Yaoming Xie, and Henry F. Schaefer, III*

Contribution from the Center for Computational Quantum Chemistry, University of Georgia, Athens, Georgia 30602. Received July 2, 1990

Abstract: Second-row analogues of N_2O have been the subjects of several recent studies. Reported here are ab initio theoretical geometries and vibrational frequencies for the N_2O analogue P_2O. These results were obtained at higher levels of theory than previously reported. We also report ab initio theoretical results for the isomers of protonated P_2O. Although the second-row atoms strongly affect the electronic structure and lower the relative energy of the cyclic isomer, the linear isomer remains the global minimum for the P_2O molecule. However, it is found that protonation of P_2O reverses the relative energies of the cyclic and linear isomers. Protonated (either phosphorus- or oxygen-protonated) cyclic P_2O is predicted to be lower in energy than protonated linear P_2O by about 11 kcal mol^{-1}. This leads us to postulate cyclic structures for isoelectronic species, including P_2CH_2 and P_2NH, and to quantitatively predict a cyclic structure for P_2F^+, based on ab initio results.

Introduction

Several important recent papers have reported the isolation of second- (long) row analogues of N_2O, including PNO,[1] N_2S,[2,3] and P_2O.[4,5] Andrews and Withnall reported P_2O as a probable product of the reaction of P_4 and oxygen atoms and assigned an IR frequency of 1192 cm^{-1} to the P=O stretch in an argon matrix.[4] Further experimental studies by Mielke, McCluskey, and Andrews[5] reassigned the P=O stretch to 1270 cm^{-1}. The various reaction products proposed by these experimental studies, including P_2O, have been examined theoretically by Jarrett-Sprague, Hillier, and Gould[6] and Lohr.[7] The geometries and electronic structures of these N_2O analogue will be strongly influenced by the poor multiple bonding ability of the second-row atoms. For example, compared to the first-row triatomics, the cyclic structures are much lower in energy.[6-8] The chemistry of these triatomics should also be quite different from that of N_2O.

We have undertaken a series of studies on N_2O analogues,[9,10] and we report here results for both linear and cyclic P_2O obtained at higher levels of theory than reported previously. More importantly, we investigate the theoretical structures and vibrational frequencies of the protonated isomers of P_2O. We have used the protonation reaction to explore the bonding and reactivity of the second-row analogues of N_2O, and for P_2O we find a remarkable reversal of the relative energy of the linear and cyclic minima upon protonation. This prompted us to theoretically determine the theoretical structures of the isoelectronic P_2F^+ ion, which are reported along with their theoretical vibrational frequencies.

Methods

The standard double-zeta (DZ) and triple-zeta (TZ) basis sets of Dunning and Huzinaga[11,12] were used. Polarization functions (i.e., d

functions) with exponents of O, 0.85, and P, 0.50, were added to the DZ basis to give the double-zeta plus polarization (DZP) basis set, and two sets of polarization functions with exponents of O, 1.70 and 0.425, and P, 1.00 and 0.25, were added to the TZ basis set to give the TZ2P basis set. All geometries were obtained via analytic first derivative methods. Self-consistent field (SCF) vibrational frequencies were evaluated by analytic second derivative methods; configuration interaction singles and doubles (CISD), coupled cluster singles and doubles (CCSD), and complete active space self-consistent field (CAS-SCF) vibrational frequencies were determined by finite differences of analytic first derivatives. The SCF, CISD, and CCSD methods were those developed in our own group, and coded in the PSI suite of programs.[13] The CAS-SCF method was that of Werner and Knowles.[14] The CAS-SCF active space included the 2s and 2p orbitals for first-row atoms, and the 3s and 3p orbitals for second-row atoms. Thus, the active space for P_2O included 16 electrons in 12 molecular orbitals.

Results and Discussion

The structures of the linear $^1\Sigma^+$ and the cyclic $^1A_1$ and $^3B_2$ states of P_2O are given in Figure 1. The theoretical vibrational frequencies and total energies of the same three states are given in Table I. The theoretical structures of the protonated isomers are given in Figure 2, a (singlet states) and b (triplet states). The singlet protonated isomers are either $^1A'$ (C_s symmetry) or ^1A (C_1 symmetry) electronic states. The theoretical vibrational frequencies and total energies of the singlet protonated isomers are given in Table II. The relative energies of the nonprotonated and protonated structures at various levels of theory are given in Tables III and IV, respectively.

Molecular orbital diagrams of the valence orbitals for both linear and cyclic P_2O are given in Figure 3. These diagrams are based qualitatively on the DZP SCF molecular orbitals. The π molecular orbitals of linear P_2O reflect the weakness of the P–P π bond. The P–P π bonding molecular orbital is at higher energy than the oxygen 2p atomic orbital; therefore, the lower, totally in-phase π orbital is polarized toward oxygen, and the higher, P–P bonding, P–O antibonding π orbital is polarized toward the outer phosphorus.
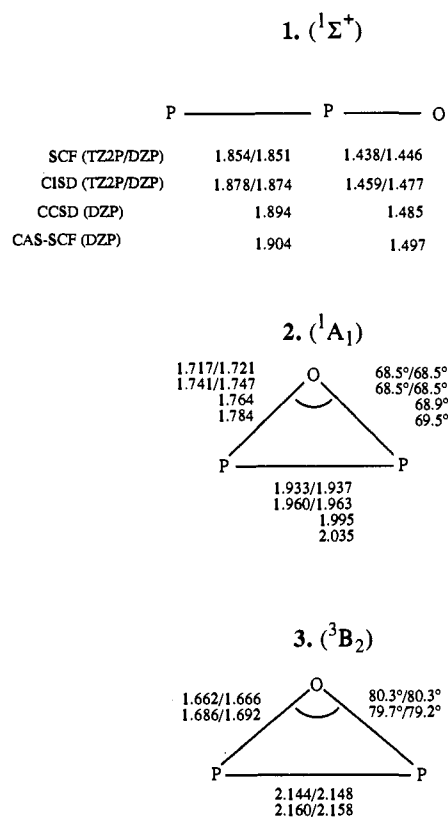
The weakness of the π bonding in this molecule makes electron correlation essential for a reliable theoretical description of the structure and vibrational frequencies. At the DZP SCF level, the theoretical PO stretching frequency of P_2O is about 13% higher than the experimental 1270 cm^{-1}, both in our studies and those previously published.[6,7] Of the previous studies, Jarrett-Sprague and co-workers[6] reported frequencies at correlated (MP2) levels;

(1) Ahlrichs, R.; Schunck, S.; Schnöckel, H. *Angew. Chem., Int. Ed. Engl.* **1988**, *27*, 421.

(2) Bender H.; Carnovale, F.; Peel, J. B.; Wentrup, C. *J. Am. Chem. Soc.* **1988**, *110*, 3458.

(3) Wentrup, C.; Fischer, S.; Maquestiau, A.; Flammang, R. *J. Org. Chem.* **1986**, *51*, 1988.

(4) Andrews, L.; Withnall, R. *J. Am. Chem. Soc.* **1988**, *110*, 5605.

(5) Mielke, Z.; McCluskey, M.; Andrews, L. *Chem. Phys. Lett.* **1990**, *165*, 146.

(6) Jarrett-Sprague, S. A.; Hillier, I. H.; Gould, I. R. *Chem. Phys.* **1990**, *140*, 27.

(7) Lohr, L. L. *J. Phys. Chem.* **1990**, *94*, 1807.

(8) Korkin, A. A.; Mebel', A. M.; Borisov, E. V. *Bull. Acad. Sci. USSR, Div. Chem. Sci. (Engl. Trans.)* **1988**, *37*, 780.

(9) Davy R. D.; Schaefer, H. F. *J. Chem. Phys.* **1990**, *92*, 5417.

(10) Davy R. D.; Schaefer, H. F. *J. Am. Chem. Soc.* **1991**, *113*, 1917.

(11) Huzinaga, S. *J. Chem. Phys.* **1965**, *42*, 1293.

(12) Dunning, T. H. *J. Chem. Phys.* **1970**, *53*, 2823.

(13) PSI, distributed by PSITECH, Inc., Watkinsville, GA.

(14) Knowles, P. J.; Werner, H. J. *Chem. Phys. Lett.* **1985**, *115*, 259.

3698 *J. Am. Chem. Soc., Vol. 113, No. 10, 1991*

Davy et al.

Table I. Theoretical Vibrational Frequencies (in cm⁻¹) and Total Energies (in Hartrees) for the Linear $^1\Sigma^+$ State and Cyclic $^1A_1$ and $^3B_2$ States of P_2O

	SCF		CISD		CCSD	CASSCF
	DZP	TZ2P	DZP	TZ2P	DZP	DZP
1, Linear $^1\Sigma^+$						
ω_1 σ^+ (P=O stretch)	1435	1438	1365	1366	1306	1264
ω_2 σ^+ (P=P stretch)	758	750	721	707	684	637
ω_3 π (PPO bend)	233	257	151	231	191	189
$E(-756.+)$	−0.26102	−0.28526	−0.72950	−0.82852	−0.83988	−0.41075
			−0.78916^a	−0.89791^a		
2, Cyclic $^1A_1$						
ω_1 a_1 (PO+PO+PP)	922	916	868	861	819	752
ω_2 a_1 (2PP−PO−PO)	736	745	690	695	630	541
ω_3 b_2 (+PO−PO)	286	244	268	232	271	154i
$E(-756.+)$	−0.24771	−0.26535	−0.71804	−0.81135	−0.83136	−0.38964
			−0.77885^a	−0.88214^a		
3, Cyclic $^3B_2$						
ω_1 a_1 (PO+PO+PO)	95	933				
ω_2 a_1 (2PP−PO−PO)	660	643				
ω_3 b_2 (+PO−PO)	557	558				
$E(-756.+)$	−0.27056	−0.28518	−0.72306	−0.81537		
			−0.77699^a	−0.87997^a		

^{a} Includes Davidson's correction for unlinked quadruple excitations.

1. ($^1\Sigma^+$)

P ———————— P ———————— O

SCF (TZ2P/DZP)	1.854/1.851	1.438/1.446
CISD (TZ2P/DZP)	1.878/1.874	1.459/1.477
CCSD (DZP)	1.894	1.485
CAS-SCF (DZP)	1.904	1.497

2. ($^1A_1$)

1.717/1.721
1.741/1.747
1.764
1.784

68.5°/68.5°
68.5°/68.5°
68.9°
69.5°

1.933/1.937
1.960/1.963
1.995
2.035

3. ($^3B_2$)

1.662/1.666
1.686/1.692

80.3°/80.3°
79.7°/79.2°

2.144/2.148
2.160/2.158

Figure 1. Theoretical geometries in ångströms and degrees for the liner $^1\Sigma^+$, cyclic $^1A_1$ and cyclic $^3B_2$ isomers of P_2O.

the DZP MP2 vibrational frequency was 1303 cm⁻¹, which is within 3% of the later experiment.[5] Our results also support 1270 cm⁻¹ as the better value; at the DZP CISD level the ω_1 stretching frequency is about 7.5% greater, and at the CCSD level only about 3% greater than 1270 cm⁻¹. Although the CAS-SCF method recovers only a fraction of the correlation energy obtained by the CISD or CCSD methods, the theoretical stretching frequency is very close to the experimental value. The very close match is fortuitous, but it shows the importance of valence correlation effects in reducing the SCF overestimation of stretching vibrational frequencies in weak multiple bonds.

Our SCF results for the $^1A_1$ state of cyclic P_2O are close to those reported previously.[6,7] Jarrett-Sprague suggested that the IR line observed at 856 cm⁻¹ might be an A_1 vibrational fre-

quencies at the CISD, CCSD, and CAS-SCF levels. The trend for the ring breathing mode is to decrease both with larger basis sets, and with increasing electron correlation. We would expect the true frequency to be below the theoretical frequency of 819 cm⁻¹ (DZP CCSD), and should probably not be assigned to the experimental line at 856 cm⁻¹.

The HOMO of cyclic P_2O (see Figure 3) is of b_1 symmetry (a P−O antibonding, P−P bonding π orbital), and the LUMO is the a_2 symmetry P−P π antibonding orbital. Because the HOMO is P−O antibonding, it is high lying, and because the P−P π bond is weak, the LUMO is low lying. This indicates the possibility of a low-energy $^3B_2$ excited electronic state with an orbital occupation ...(3b_1)(2a_2). One might also expect this possibility based on the isoelectronic P_3^- ion, which has a low-lying triplet excited electronic state.[15] Table III shows that the $^3B_2$ state is of higher energy than the $^1A_1$ state, but only when Davidson's correction[16] for unlinked quadruple excitations is added to the CISD energy (CISD + Q). The energies of the cyclic states relative to the $^1\Sigma^+$ state vary markedly with electron correlation and basis set. Our best estimate for the $^1\Sigma^+$ − $^1A_1$ energy difference is 8.7 kcal mol⁻¹, based on the DZP CCSD energy difference (5.3 kcal mol⁻¹) plus the effect of basis set at the CISD + Q level [(TZ2P CISD + Q) − (DZP CISD + Q)] = 3.4 kcal mol⁻¹. At the highest level actually investigated (TZ2P CISD + Q), the $^3B_2$ state was only 1.4 kcal mol⁻¹ higher than the $^1A_1$ state.

The effect of protonation of P_2O is a striking reversal of the energy minima on the singlet surface. Both P- and O-protonated isomers of cyclic P_2O are lower in energy than either P- or O-protonated linear P_2O. Viewed another way, the protonation energy of the cyclic isomer is much greater (by more than 20 kcal mol⁻¹ at the DZP CISD level) than the protonation energy of the linear isomer. This is the most important finding of the present research.

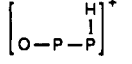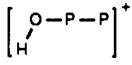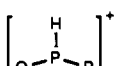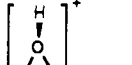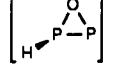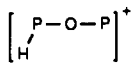From the molecular orbital diagram given in Figure 3, we see, as noted before, that the HOMO of the linear P_2O is polarized toward the terminal phosphorus. Thus, one might expect protonation to occur preferentially at phosphorus and write resonance structure (A) with P−P and P−O double bonds:

$$\overset{\displaystyle H}{\underset{\displaystyle}{\overset{..}{O}=\overset{+}{P}=P}}$$

A
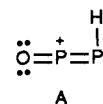
The electronegativity of oxygen, however, gives P_2O a substantial

(15) Hamilton, T. P.; Schaefer, H. F. *Chem. Phys. Lett.* **1990**, *166*, 303.
(16) Davidson, E. R. In *The World of Quantum Chemistry*; Daudel, R., Pullman, B., Eds.; Reidel: Dordrecht, 1974; pp 17–30.
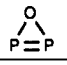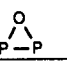
Cyclic Global Minimum of HP₂O⁺

J. Am. Chem. Soc., Vol. 113, No. 10, 1991 3699

Table II. Theoretical Vibrational Frequencies (cm⁻¹) and Total Energies (in Hartrees) for the Lowest Singlet State of Various Protonated P₂O Isomers

assignment	SCF DZP	SCF TZ2P	CISD DZP
$\left[\begin{smallmatrix} & & H \\ & & | \\ O & - P & - P \end{smallmatrix}\right]^+$ (4)			
ω₁ a′ (PH stretch)	2419	2389	2381
ω₂ a′ (PO stretch)	1546	1550	1447
ω₃ a′ (PP stretch − HPP bend)	747	772	716
ω₄ a′ (PP stretch + HPP bend)	525	530	520
ω₅ a′ (PPO bend)	182	207	156
ω₆ a″ (torsion)	134	189	147
energy	−756.51431	−756.54486	−756.99163 −757.05394[a]
$\left[\begin{smallmatrix} O - P - P \\ / \\ H \end{smallmatrix}\right]^+$ (5)			
ω₁ a′ (OH stretch)	3989	3967	3863
ω₂ a′ (PO stretch)	1240	1241	1172
ω₃ a′ (POH bend)	907	930	908
ω₄ a′ (PP stretch)	737	727	693
ω₅ a″ (torsion)	113	136	111
ω₆ a′ (PPO bend)	55	85	72
energy	−756.55056	−756.57342	−757.02052 −757.08053[a]
$\left[\begin{smallmatrix} & H \\ & | \\ O - P & - P \end{smallmatrix}\right]^+$ (6)			
ω₁ a′ (PH stretch)	2590	2578	2544
ω₂ a′ (PO stretch)	1458	1464	1358
ω₃ a′ (OPH bend)	1018	1005	969
ω₄ a″ (out-of-plane)	570	583	521
ω₅ a′ (PP stretch)	526	530	532
ω₆ a′ ((PPH–PPO) bend)	221	209	185
energy	−756.50014	−756.52717	−756.95999 −757.01707[a]
$\left[\begin{smallmatrix} & H \\ & | \\ & O \\ P & - P \end{smallmatrix}\right]^+$ (7)			
ω₁ a′ (OH stretch)	3990	3997	3838
ω₂ a″ ((POH–POH) bend)	1000	1024	971
ω₃ a′ (H out-of-plane)	987	1032	998
ω₄ a′ ((PP+PO+PO) stretch)	822	819	778
ω₅ a′ ((2PP–PO–PO) stretch)	693	690	652
ω₆ a″ ((PO–PO) stretch)	311	306	360
energy	−756.56653	−756.58712	−757.03855 −757.09909[a]
$\left[\begin{smallmatrix} & O \\ & / \\ H & P - P \end{smallmatrix}\right]^+$ (8)			
ω₁ (PH stretch)	2541	2527	2508
ω₂ (PO stretch)	1152	1139	1105
ω₃ ((OPH+PPH) bend)	1022	1005	976
ω₄ ((OPH–PPH) bend)	755	749	719
ω₅ (PO stretch)	573	552	544
ω₆ (PP stretch)	512	512	490
energy	−756.57010	−756.59197	−757.03907 −757.09792[a]
$\left[\begin{smallmatrix} P - O - P \\ / \\ H \end{smallmatrix}\right]^+$ (9)			
ω₁ a′ (PH stretch)	2541	2528	2530
ω₂ a′ (OPH bend)	1151	1148	1111
ω₃ a′ (PO stretch)	970	951	902
ω₄ a′ (PO stretch)	549	539	571
ω₅ a″ (POPH torsion)	286	268	323
ω₆ a′ (POP bend)	180	137	220
energy	−756.52827	−756.53839	−756.99555 −757.05895[a]

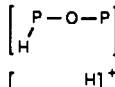[a] Included Davidson's correction for unlinked quadruple excitations.
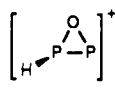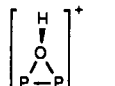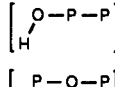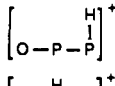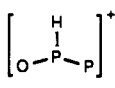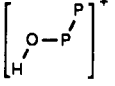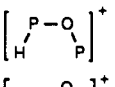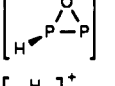
dipole moment (2.33 D at the DZP CISD level). Presumably the greater electron density at oxygen makes PPOH⁺ the lower energy isomer. Much of the electron density at oxygen, however, is due to the 2π bonding orbital. Protonation at oxygen weakens the

Table III. Relative Energies of Linear ¹Σ⁺ and Cyclic ¹A₁ and ³B₂ States of P₂O (kcal mol⁻¹)

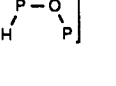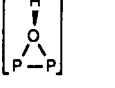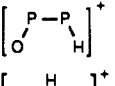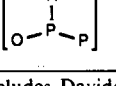|	1, ¹Σ⁺ P=P=O	2, ¹A₁ $\overset{O}{\underset{P=P}{\triangle}}$	3, ³B₂ $\overset{O}{\underset{P-P}{\triangle}}$
SCF			
DZP	0.0	8.4	−6.0
TZ2P	0.0	12.5	0.1
CISD			
DZP	0.0	7.2 (6.5)[a]	4.0 (7.6)[a]
TZ2P	0.0	10.8 (9.9)[a]	8.3 (11.3)[a]
CCSD			
DZP	0.0	5.3	
CAS-SCF			
DZP	0.0	13.2	

[a] Includes Davidson's correction for unlinked quadruple excitations.

Table IV. Relative Energies of Various Singlet-State and Triplet-State Isomers of Protonated P₂O (in kcal mol⁻¹)

| structure	SCF DZP	SCF TZ2P	CISD DZP
(a) Singlet-State Isomers			
8 $\left[\begin{smallmatrix} O \\ / \triangle \\ H & P - P \end{smallmatrix}\right]^+$	0.0	0.0	0.0 (0.0)[a]
7 $\left[\begin{smallmatrix} H \\ | \\ O \\ \triangle \\ P - P \end{smallmatrix}\right]^+$	2.2	3.0	0.3 (−0.7)[a]
5 $\left[\begin{smallmatrix} O - P - P \\ / \\ H \end{smallmatrix}\right]^+$	12.3	11.6	11.6 (10.9)[a]
9 $\left[\begin{smallmatrix} P - O - P \\ / \\ H \end{smallmatrix}\right]^+$	26.3	33.6	27.3 (24.5)[a]
4 $\left[\begin{smallmatrix} & H \\ & | \\ O - P - P \end{smallmatrix}\right]^+$	35.0	29.6	29.8 (27.6)[a]
6 $\left[\begin{smallmatrix} & H \\ & | \\ O - P - P \end{smallmatrix}\right]^+$	43.9	40.7	49.6 (50.7)[a]
(b) Triplet-State Isomers			
5 $\left[\begin{smallmatrix} P \\ / \\ O - P \\ | \\ H \end{smallmatrix}\right]^+$	−11.5 −8.7	−10.3	3.3 (7.7) (trans) (cis)
9 $\left[\begin{smallmatrix} P - O \\ / & \backslash \\ H & P \end{smallmatrix}\right]^+$	−7.8 −7.3	−1.6	7.8 (12.6) (cis) (trans)
8 $\left[\begin{smallmatrix} O \\ / \triangle \\ H & P - P \end{smallmatrix}\right]^+$	collapses to $\left[\begin{smallmatrix} P - O \\ / & \backslash \\ H & P \end{smallmatrix}\right]^+$		
7 $\left[\begin{smallmatrix} H \\ | \\ O \\ \triangle \\ P - P \end{smallmatrix}\right]^+$	6.2	10.7	17.9 (21.6)
4 $\left[\begin{smallmatrix} P - P \\ / & \backslash \\ O & H \end{smallmatrix}\right]^+$	7.8 8.2	9.1 9.4	18.4 (20.6) (cis) 18.8 (21.1) (trans)
6 $\left[\begin{smallmatrix} & H \\ & | \\ O - P - P \end{smallmatrix}\right]^+$	14.1	12.5	25.3 (28.3)

[a] Includes Davidson's correction for unlinked quadruple excitations.

P–O bond; in effect protonation shifts multiple bond character from the P–O bond to the P–P bond, as reflected in the resonance structure (B):

$$O - \overset{+}{P} \equiv P:$$
$$\underset{H}{|}$$

B
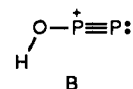
and in the 0.010–0.015-Å decrease in the theoretical P–P distance. The weakness of the P–P (formally) triple bond is indicated by

3700 *J. Am. Chem. Soc., Vol. 113, No. 10, 1991*

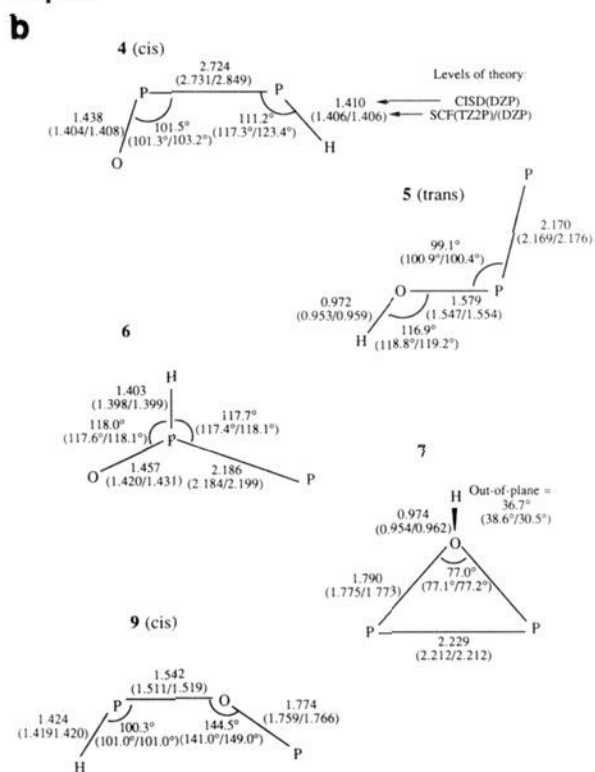*Davy et al.*

Singlet

a

Triplet

b
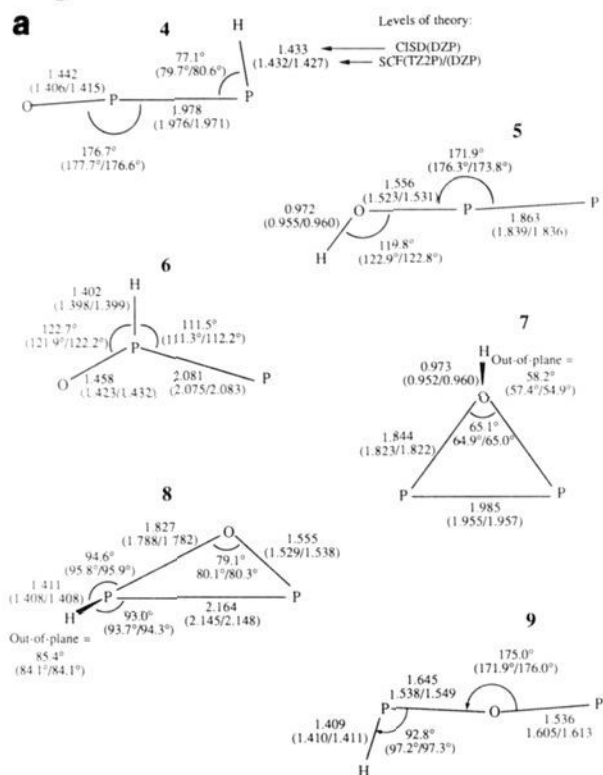
Figure 2. Theoretical geometries for the lowest singlet state (a) and lowest triplet state (b) of various protonated P_2O isomers. All bond distances are in Å.

the low PPO bending frequency of PPOH$^+$ (72 cm^{-1} at the DZP CISD level).

The energies of P- and O-protonated cyclic P_2O structures differ by only 3.0 kcal mol^{-1} at the DZP SCF level, and by less than 1 kcal mol^{-1} at the DZP CISD level. Electron correlation lowers
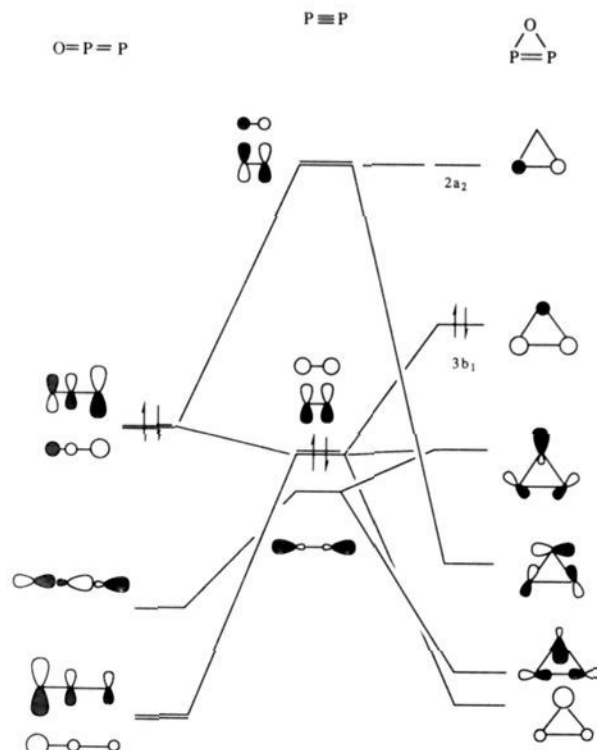

Figure 3. Qualitative molecular orbital diagram (based on DZP SCF orbitals) for linear and cyclic P_2O.

Table V. Total Energies (hartrees) and Theoretical Vibrational Frequencies (cm^{-1}) for Bent and Cyclic P_2F^+

assignment	SCF		CISD	
	DZP	TZ2P	DZP	TZ2P
		$\overset{F}{\underset{P-P}{\diagup\diagdown}}$		
ω_1 (PF+PF+PF)	802	801	762	
ω_2 (2PP−PF−PF)	662	657	633	
ω_3 (PF−PF)	33i	81i	230	
energy	−780.53056	−780.55156	−780.99465	−781.16763
			−781.05197[a]	−781.23907[a]
		$\overset{F}{\underset{P-P}{\vert}}$		
ω_1 (PF stretch)	964	954	895	
ω_2 (PP stretch)	621	614	599	
ω_3 (bend)	192	184	172	
energy	−780.53978	−780.56156	−780.98884	−781.16452
			−781.04186[a]	−781.23202[a]

[a] Includes Davidson's correction for unlinked quadruple excitations.

the relative energy of the O-protonated isomer, but improved basis set (at the SCF level) favors the P-protonated isomer. Under any extrapolation, therefore, the two isomers should remain nearly isoenergetic.

Triplet States

Following a referee's suggestion, a search for low-lying triplet electronic states was also carried out. These results are summarized in Figure 2b and Table IVb. Some of these structures are quite low lying energetically. In particular, the triplet trans HOPP$^+$ structure 5 is predicted to lie only 7.7 kcal/mol above the global minimum, cyclic singlet state 8. In Figure 2b, only the lower energy structure (either cis or trans) is displayed when a second geometrical isomer exists.

Related Systems

Protonation of the cyclic isomer stabilizes the 3b$_1$ P−O antibonding orbital, in contrast to linear P_2O, in which the proton interacts with nonbonding or even bonding orbitals. If one completely removed the 3b$_1$ electrons, then cyclic P_2O would have two
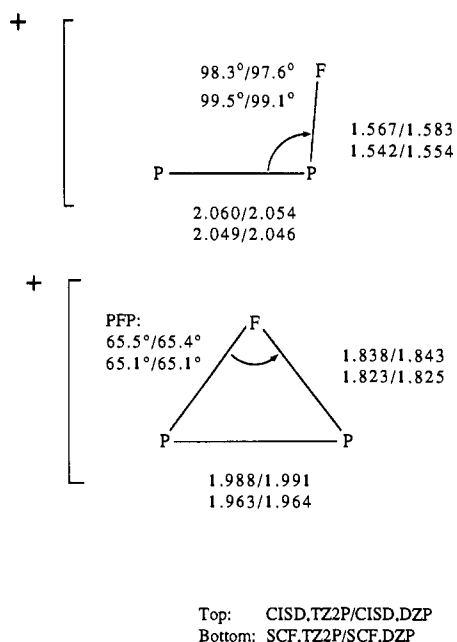
Top: CISD,TZ2P/CISD,DZP
Bottom: SCF,TZ2P/SCF,DZP

Figure 4. Theoretical geometris in ångströms and degrees for the bent and cyclic isomers of P_2F^+.

ring electrons, fulfilling the $4n + 2$ rule. Thus one would also predict P_2O^{2+} and P_2N^+ to be cyclic. Protonation at phosphorus weakens the P–P bond and the P_H–O bond substantially and shortens the P–O bond. One gives up P–P multiple bonding to gain P–O multiple bonding. Protonation at oxygen also strengthens the P–O bonds and weakens the P–P bond.

Another way to weaken the antibonding $3b_1$ interaction is to replace oxygen by fluorine. The energy of the fluorine atomic p orbital would be even further below the P–P π bonding orbital than the oxygen p orbital. If weakening the ring π interaction favors the cyclic structure, one might expect P_2F^+ to be cyclic. This hypothesis was tested theoretically by optimizing the structures of the isoelectronic P_2F^+. We found two stationary points, which are shown in Figure 4: a bent structure and a cyclic structure. The total energies and theoretical vibrational frequencies are given in Table V, and the relative energies are given in Table VI. At the SCF level, the bent structure is a minimum, and the cyclic structure is a transition state between the two equivalent bent structures. When correlation is included, however,

Table VI. Relative Energies of Bent and Cyclic P_2F^+ (kcal mol^{-1})

	SCF		CISD	
	DZP	TZ2P	DZP	TZ2P
F | P—P	0.0	0.0	0.0	0.0
F /\\ P—P	5.8	6.3	-3.4 -6.3[a]	-2.0 -4.4[a]

[a] Includes Davidson's correction for unlinked quadruple excitations.

the cyclic structure is not only a minimum, it is the global minimum, 4.4 kcal mol^{-1} below the bent structure at the TZ2P CISD + Q level.

The linear structure was also a transition state at the DZP SCF level and was not investigated further. The highly electronegative fluorine will not form the linear structure (C), presumably because it would force a P–P triple bond:

$$:P{\equiv}\overset{+}{P}{-}\overset{\cdot\cdot}{\underset{\cdot\cdot}{F}}:$$

C
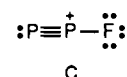
Viewed in terms of resonance structures, both cyclic and bent P_2F^+ contain ionic terms:

$$\overset{\cdot\cdot}{\underset{\cdot\cdot}{:F:}}{}^{-} \qquad \overset{\cdot\cdot}{\underset{\cdot\cdot}{:F:}}{}^{-}$$
$$:P{=}P:\qquad :P{=}P:$$
$$2+\qquad\qquad 2+$$

This is shown by the Mulliken populations which have a negative charge on the fluorine (–0.44 and –0.40 for cyclic and bent, respectively, at the TZ2P CISD level of theory).

If the key to stabilizing the cyclic structure is the weakening of the b_1 antibonding orbital interaction, one might expect that the groups NH and CH_2, which are isoelectronic to OH^+, might also prefer cyclic structures to linear ones when attached to P_2. In these cases the b_1 interaction would be weakened because the N–H and C–H bonds would polarize the N or C p_x orbital away from the phosphorus π orbitals. Although ring-opening polymerizations would certainly be energetically favored, if one could isolate these molecules (P_2F^+, P_2CH_2, or P_2NH) either in the gas phase, or in an inert matrix, they hold promise of being stable three-membered rings incorporating a P–P double bond.

Twisted Double Bond in Methylenephosphonium Ions. A Theoretical Investigation

Michael Ehrig, Hans Horn, Christoph Kölmel, and Reinhart Ahlrichs*

Contribution from the Lehrstuhl für Theoretische Chemie, Institut für Physikalische Chemie und Elektrochemie, Universität Karlsruhe, D-7500 Karlsruhe, Federal Republic of Germany.
Received August 8, 1990

Abstract: Results of rigorous SCF calculations, including structure optimizations, are reported for $(R_2N)_2P^+{=}C(SiR'_3)_2$: R = H, Me, *i*-Pr; R' = H, Me (and for $R_2P^+{=}CR'_2$ for comparison). Twisting of the $P^+{=}C$ double bond caused by steric hindrance of bulky groups R and R' is facilitated by the electronic structure of the parent compound $(H_2N)_2P^+{=}C(SiH_3)_2$ which differs markedly from the genuine double-bond structure found in $H_2P^+{=}CH_2$.

I. Introduction

Igau, Baceiredo, Grützmacher, Pritzkow, and Bertrand[1] have recently reported the synthesis and crystal structure of the me-

thylenephosphonium ion 1, with R = *i*-Pr (C_3H_7) and R' = Me with $CF_3SO_3^-$ as counterion. 1 could be simply considered as a phosphanylcarbene 2, and the basic question addressed in the present work concerns the specific importance of amino and silyl groups for the properties of 1.

The crystal structure of 1, visualized in Figure 1a, shows re-

(1) Igau, A.; Baceiredo, A.; Grützmacher, H.; Pritzkow, H.; Bertrand, G. *J. Am. Chem. Soc.* **1989**, *111*, 6853.